Version dated: January 30, 2017

So many genes, so little time: comments on divergence-time estimation in the genomic era

Stephen A. Smith[1], and Joseph W. Brown[1†], Joseph F. Walker[1†]

[1]*Department of Ecology and Evolutionary Biology, University of Michigan, Ann Arbor, Michigan, 48109, USA*

[†]*Equal contribution*

Corresponding author: Stephen A. Smith, Ecology and Evolutionary Biology, University of Michigan, Ann Arbor, Michigan, 48109, USA; E-mail: eebsmith@umich.edu.

Abstract

1. Phylogenomic datasets have emerged as an important tool and have been used for addressing questions involving evolutionary relationships, patterns of genome structure, signatures of selection, and gene and genome duplications. Here, we examine these data sources for their utility in divergence-time analyses. Divergence-time estimation can be complicated by the heterogeneity of rates among lineages and through time. Despite the recent explosion of phylogenomic data, it is still unclear what the distribution of gene- and lineage-specific rate heterogeneity is over these genomic and transcriptomic datasets.

2. Here, we examine rate heterogeneity across genes and determine whether clock-like or nearly clock-like genes are present in phylogenomic datasets that could be used to reduce error in divergence-time estimation. We address these questions with six

published phylogenomic datasets including Birds, carnivorous Caryophyllales, broad Caryophyllales, Millipedes, Hymenoptera, and Vitales. We introduce a simple and fast method for identifying useful genes for constructing divergence-time estimates and conduct exemplar Bayesian analyses under both clock and uncorrelated log-normal (UCLN) models.

3. We used a "gene shopping" method (implemented in `SortaDate`) to identify genes with minimal conflict, lower root-to-tip variance, and discernible amounts of molecular evolution. We find that every empirical dataset examined includes genes with clock-like, or nearly clock-like, behavior. Many datasets have genes that are not only clock-like, but also have reasonable evolutionary rates and are mostly compatible with the species tree. We used these data to conduct basic divergence-time analyses under strict clock and UCLN models. These exemplar divergence-time analyses show overlap in age estimates when using either clock or UCLN models, but with much larger credibility intervals for UCLN models.

4. We find that "gene shopping" can be productive and successful in finding gene regions that minimize lineage-specific heterogeneity. By doing relatively simple assessments of root-to-tip variance and bipartition conflict, we not only explore datasets more thoroughly but also may estimate ages on phylogenies with lower error. We also suggest the need to explore more detailed and informative approaches to determine fit and deviation from a molecular clock, as existing approaches are exceedingly strict.

Introduction

Datasets based on thousands of genes from genomes and transcriptomes have emerged as a major tool in addressing broad evolutionary questions including, but not limited to, phylogenetic reconstruction, gene and genome duplication, and inference of molecular evolutionary patterns and processes. And while these datasets have been used for divergence-time estimation (e.g., Jarvis *et al.* 2014b; Prum *et al.* 2015), their overall utility

for divergence-time analyses has not been fully examined. In particular, it is unclear whether within these enormous datasets there exist nearly clock-like gene regions that may aid in producing lower error divergence-time estimates. While some authors, such as Jarvis *et al.* (2014b), have suggested choosing clock-like genes, a repeatable and fast procedure to identify these genes has not been developed for phylogenomics and an examination of the frequency of these genes in empirical datasets has not been conducted.

Divergence-time estimation is a complicated, but often essential, step for many phylogenetic analyses. The sources of error include the ambiguous nature of fossil placement, significant variation in the branchwise rates of evolution, significant variation in the sitewise rates of evolution, uncertainty in the phylogenetic tree, topological dissonance amongst gene trees due to incomplete lineage sorting, and complexity of the model for the molecular clock (e.g., Smith *et al.* 2010; Dornburg *et al.* 2012; Parham *et al.* 2012; Beaulieu *et al.* 2015). While fossils give the only available information for absolute age, their placement and age carry uncertainty. Multiple fossil calibrations and complicated tree shape priors can interact to further complicate molecular dating (Zhu *et al.* 2015; Heled and Drummond 2015). Rate variation is common among individual branches and across sites and can contribute to extensive deviations from the molecular clock. As a result, complex models have been developed to accommodate for these deviations (Sanderson 2002; Drummond *et al.* 2006; Drummond and Suchard 2010). However, these more parameter-rich models also carry with them significant uncertainty and can, when the data deviate significantly from the model, positively bias results (e.g., Worobey *et al.* 2014). Despite these difficulties, researchers continue to use divergence-time estimates extensively as they remain essential for many downstream evolutionary and comparative analyses.

Researchers can take steps to ease sources of errors for divergence-time analyses. For example, better use of fossils in temporal calibrations can dramatically improve estimations (e.g., Parham *et al.* 2012; Ksepka *et al.* 2015), as does better accounting for rate variation in the molecular models by improving model fit. Several relaxed clock models have been introduced over the last few decades to accommodate rate heterogeneity

because most data do not conform to a strict clock. The most commonly used relaxed clock models include penalized likelihood (PL, Sanderson 2002) as implemented in `r8s` (Sanderson 2003) and `treePL` (Smith and O'Meara 2012), and the uncorrelated lognormal model (UCLN) as implemented in `BEAST` (Drummond and Rambaut 2007). This is not an exhaustive list as other methods have been developed and new ones are continually released (e.g., Lepage *et al.* 2007; Tamura *et al.* 2012; Heath *et al.* 2014). The diversity of techniques is matched with a variety of different inputs. For example, PL implementations minimally require an estimated phylogram, calibration, smoothing penalty value, and alignment size, while Bayesian estimation in `BEAST` minimally requires an alignment and priors to be set for each parameter, including any fossil calibrations.

Bayesian methods that use the UCLN model of rate variation (Drummond *et al.* 2006), such as that implemented in `BEAST`, simultaneously estimate phylogenetic relationships and divergence times, and so may be preferred over PL approaches as BEAST incorporates uncertainty more easily and explicitly. However, the computational burden of these simultaneous reconstruction methods limit their use to smaller datasets (i.e., not the entire genome or transcriptome). By "gene shopping" for genes that best conform to a molecular clock or relaxed molecular clock we can reduce larger datasets to datasets that are capable of being analyzed with BEAST or other programs. Before the recent development of next-generation sequencing techniques, this was not possible because of the relatively small number of genes available for any single clade. However, as genomic and transcriptomic datasets have become more readily available, "gene shopping" has become a potentially fruitful approach for divergence-time estimation (e.g., Jarvis *et al.* 2014b). Nevertheless, the utility of these large genomic datasets for divergence-time estimation and the distribution of lineage-specific rate heterogeneity has yet to be fully explored.

Next generation sequencing techniques have dramatically increased the number of gene regions available for phylogenetic analysis. This has stimulated research into questions that are specifically pertinent to datasets with hundreds or thousands of genes. What is the best method for reconstructing the species tree (e.g., Gatesy and Springer 2014;

Mirarab *et al.* 2014; Roch and Warnow 2015)? How many genes support the dominant species tree signal (e.g., Salichos *et al.* 2014; Smith *et al.* 2015)? Genomic datasets also allow us to examine the extent of molecular rate variation in genes, genomes, and lineages (Jarvis *et al.* 2014b; Yang *et al.* 2015). For example, Yang *et al.* (2015) explored the distribution of lineage-specific rate heterogeneity throughout transcriptomes of the plant clade Caryophyllales as it relates to life history, and Jarvis *et al.* (2014b) explored rate heterogeneity and selection as it relates to errors in phylogeny reconstruction in a genomic dataset of birds. Jarvis *et al.* (2014b) also filtered gene regions to identify "clock-like" genes for divergence-time estimation. While Jarvis *et al.* (2014b) conducted a filtering analysis on their genomic data, a thorough examination of lineage-specific rate heterogeneity for divergence-time estimation has not been conducted. Nevertheless, the availability of full genomes and transcriptomes makes identifying genes with lower rate variation possible and so are more suitable for divergence-time estimation.

Here, we examine six genomic and transcriptomic datasets across animals and plants and with different temporal and taxonomic scopes to examine the extent of lineage-specific rate heterogeneity. We investigate the distribution of variation in the branchwise rates of evolution across thousands of genes to understand whether these new genomic resources may improve divergence-time estimation by allowing for simpler models of molecular evolution. Finally, we introduce a simple sorting procedure to identify informative and nearly clock-like genes. This procedure can be used to examine the overall distribution of evolution, rate heterogeneity, bipartition concordance, and potential utility of genes for divergence-time analysis.

Materials and Methods

Dataset processing.— We used six published datasets to examine rate heterogeneity: Birds (BIR, Jarvis *et al.* 2014b), carnivorous Caryophyllales (CAR, Walker *et al.* 2017), the broader Caryophyllales (CARY, Yang *et al.* 2015), Vitales (VIT, Wen *et al.* 2013), Hymenoptera (HYM, Johnson *et al.* 2013), and Millipedes (MIL, Brewer and Bond 2013).

The range in datasets spans different taxonomic groups, datasets sizes (e.g., CAR vs CARY), and age (e.g., from hundreds of millions of years to within the last hundred million years). Where possible, we used orthologs that were identified using the Maximum Inclusion method of Yang and Smith (2015). This was the case with every dataset but BIR for which we used the exon alignments available online (Jarvis *et al.* 2014a; http://gigadb.org/dataset/101041). For each ortholog we have an estimated gene tree, based on maximum likelihood (ML) analyses, and alignments, from the original studies. Gene trees, regardless of the source of orthologs, were then rooted and SH-like tests were performed to assess confidence in edges (Anisimova and Gascuel 2006).

Gene tree analyses.— Because deviation from the clock is empirically manifest in a phylogram as variation in root-to-tip length among tips within a tree, we measured the variance of root-to-tip lengths for each tree. This was performed on each rooted ortholog, for which outgroups were removed, with the `pxlstr` program of `Phyx` package (Brown *et al.* 2017). We performed the standard clock test for each ortholog, with outgroup removed, using `PAUP*` (Swofford 2001) by calculating the ML score for a gene both with and without assuming a clock, and then performing a likelihood ratio test. In addition to assessing the clock-likeness of genes, we also compared gene tree topologies to the corresponding published species tree topology. Branch lengths were not available for some species trees. To compare the individual gene trees to their corresponding species trees, we conducted bipartition comparison analyses on each gene tree using `pxbp` from the `Phyx` package (procedure described in Smith *et al.* 2015).

Simulations.— We conducted simulations to examine expectations of rate variation given clock-like, noisy clock-like, and uncorrelated lognormal data. We first generated simulated clock-like data using `Indelible` v1.03 (Fletcher and Yang 2009) using the WAG model with 500 characters for amino acid datasets, and JC with 1500 characters for nucleotide datasets, on each of the empirical species tree topologies. For these data simulations, because the species tree often had no branch lengths available, node heights were first simulated randomly using `Indelible` and then the tree was rescaled to a height of 0.25,

0.5, or 0.75. We used the trees generated by `Indelible` to further simulate 100 noisy clock (rate=1.0, noise=0.25, and rate=1.0, noise=0.75) and uncorrelated lognormal (UCLN) trees (mean.log=-0.5, sd.log=0.5, and mean.log=-0.5, sd.log=1.0) using `NELSI` v0.21 (Ho *et al.* 2015). We note the 'noise' in `NELSI` corresponds to the standard deviation of a normal distribution with mean = 0. For the noisy clock, branch-specific rates are a sum of the global rate (here, 1.0) and a draw from this normal distribution. The simulations with noise=0.75 thus are only loosely clock-like, and serve as a comparison between the more clock-like (noise=0.25) and UCLN analyses. We used `RAxML` v8.2.3 (Stamatakis 2014) to reconstruct each of these datasets. For each simulation, we examined the rate variation and the root-to-tip length variation on the reconstructed phylograms.

While the focus of this study is not the performance of divergence-time estimation methods, we still wanted to examined an exemplar from the simulations to ascertain the variation in the results given different clock models. We used one random realization of node heights as simulated from the `Indelible` analyses as mentioned above to generate two datasets with `NELSI`. One dataset had three genes generated from a clock rate of 1 and noise at 0.25, and the other dataset had three genes generated from a UCLN model and mean.log at -0.5 and sd.log=1. As above, each amino acid gene consisted of 500 residues, while DNA genes consisted of 1500 nucleotides. For both the noisy clock-like and UCLN datasets, we conducted `BEAST` analyses with both a clock model and a UCLN model. A birth-death tree prior was used as the prior for all node heights, and runs were conducted for 10,000,000 generations with the first 10% discarded as burnin. Results were summarized using `treeannotator` from the `BEAST` package. Median node heights as well as 95% HPD node heights were compared between the simulated datasets and the tree used to generate these datasets.

Sorting and dating analyses on real data.— In addition to these analyses on simulated datasets, we conducted divergence-time analyses on a subset of the empirical datasets. Because these datasets consist of hundreds to thousands of genes, we developed a sorting procedure intended to mimic that which would be performed as a "gene shopping"

analysis. The sorting procedure relies on the root-to-tip variance statistic, bipartition calculation to determine the similarity to the species tree, and total treelength. We sorted first by the similarity to the species tree, then root-to-tip variance, and finally treelength. We limited the results to the top three genes reported from the sorting procedure. Because we filtered for genes that were consistent with the species tree, these genes were then concatenated and the topology was fixed to be consistent with the species tree. For each of these datasets, we conducted two `BEAST` analyses, one assuming a strict clock and the other assuming a UCLN model. Because specific dates were not the focus of this examination, the birth-death tree prior was used instead of fossil priors for nodes. The analyses were run for 10,000,000 generations with the first 1,000,000 discarded as burnin. As above, results were summarized using `treeannotator` from the `BEAST` package. Median node heights and 95% HPD node heights were compared between the clock and UCLN runs as the node heights on the true phylogeny are unknown.

Availability of procedures.— The analyses that were performed above can be conducted using the `SortaDate` package (with source code and instructions available at https://github.com/FePhyFoFum/sortadate). This package is written in Python and available as an Open Source set of procedures. In some cases, external programs are used (e.g., those found in the `Phyx` package) that are also Open Source and freely available.

Results and Discussion

A fundamental question for each of the empirical datasets is: are there clock-like gene regions present within the genome? Results were broad, from 0.4% of genes passing the clock test for the VIT dataset to 17% for the MIL dataset (see Table 1). The variation in the percentage of deviation from the clock may reflect dataset size and the age of the clade involved. As for size, the CAR dataset has 7 taxa that are not included in the CARY dataset but otherwise overlaps partially and has far fewer taxa in total. The CARY dataset, in addition to being much larger, also contains known shifts in life history (Yang *et al.* 2015). These differences may account for the variation between these two datasets.

As for clade age, HYM and MIL are significantly older than the other datasets, which may account for their rate variation. Nevertheless, each dataset indeed had at least a few orthologs that passed a strict clock test even if these orthologs were in the small minority.

Because passing a clock test does not necessarily indicate that the gene would be good for phylogenetic reconstruction, we also measured treelength and root-to-tip variance for each ortholog (see Figures 2-3). Clock tests are stringent in their need to conform to the clock (see below) and so by examining the root-to-tip variation and lineage-specific variation, we are more directly examining the deviation from ultrametricity. Although this is primarily descriptive and does not include a formal test, this provides an easily interpretable characterization of rate variation. We found that the datasets vary dramatically with no discernible general pattern for both root-to-tip variance and treelength. For example, the BIR dataset demonstrates very little molecular evolution as demonstrated by the short treelengths. For this dataset, we analyzed nucleotides (rather than amino acids) to maximize treelengths as Jarvis *et al.* (2014b) demonstrated low rates of evolution, especially deep in the phylogeny. However, the inferred rates of evolution (as determined by overall tree length) were still low. Given the difficulty in resolving the avian phylogeny, this pattern is perhaps to be expected (Jarvis *et al.* 2014b). This same pattern is present in the VIT dataset, though this was not explored as thoroughly in the original publication. Both the CAR and CARY datasets show a pattern of increasing variance with greater treelength (Figures 2). This contrasts with the HYM and MIL datasets that are clock-like even with longer treelengths (Figure 3). Lineage-specific rate variation in each dataset was idiosyncratic with most extreme variation in the outgroups. While outgroups were excluded for clock tests and in determining root-to-tip variance for "gene shopping", we allowed outgroups to remain for lineage-specific rate variation analyses as in the right handed plots of Figure 3. The VIT dataset was an exception with several lineages other than the outgroup having high rates. In each dataset, there were genes that fell within the distribution of simulated trees that are clock-like or clock-like with low noise.

One potential benefit of identifying orthologs with lower lineage-specific rate

variation within phylogenomic datasets is to use these, or a subset of these, orthologs to conduct divergence-time analyses. The hope is that by using clock-like genes, we may overcome or lessen the impact of lineage-specific rate variation on the error of divergence time analyses. The non-identifiability of rates and dates (e.g., longer branch lengths may be the result of a long time or fast evolution) is exacerbated by lineage-specific rate heterogeneity. We used a subset of orthologs to conduct divergence time analyses and we implemented a sorting procedure (packed in `SortaDate`) to (i) filter the genes that best reflect the species tree (i.e., higher bipartition concordance witht he species tree), (ii) have lower root-tot-ip variance (i.e., most clock-like), and discernible amounts of molecular evolution (i.e., greater tree length; Figure 1). For each empirical dataset, we generated such an alignment (see Table 2). The genes that were filtered and used for divergence-time analyses for the BIR, CARY, VIT, and HYM datasets rejected the clock. The genes for the CAR and MIL datasets either didn't or weakly rejected the clock. Resulting HPD trees were rescaled so that the root heights were equivalent to allow for easier comparisons between datasets. Typically, fossil placements would be used for scaling but because these are not intended to be runs for future use, we eliminated fossil placements as one source of variation. We found rough correspondence of node heights between the clock and UCLN analyses, especially for the four smallest datasets (see Figure 4). The UCLN analyses, as expected, had far greater variance in the 95% HPDs for node ages. We found the greatest differences in the larger BIR and CARY datasets (see Table 3). For both datasets, we saw major differences in tree heights, especially for CARY. This may reflect the size of the dataset or the underlying rate variation in the datasets. In general, strict clock estimates resulted in younger median node ages than analogous UCLN estimates, as well as younger maximum and older minimum 95% HPD values (see Table 3). The covariance statistics for UCLN runs ranged from the lowest mean values of -0.002 (stdev=0.04) in MIL to the highest of 0.246 (stdev=0.12) in BIR.

As is always the problem with real datasets, the true divergence-times are unknown. So we conducted exemplar analyses. For each empirical dataset, we simulated data for

three genes under both noisy clock and UCLN models to examine the variation in the resulting divergence-time analyses where the true dates were known. For these simulated datasets, a strict clock was rejected in each case, including those datasets that were simulated under a clock with noise. We compared the resulting node heights from the divergence time analyses under clock and UCLN models with the tree used for simulation (see Tables 4-5 and Figure 5). For the datasets generated under a noisy clock model, more of the true node heights were found in the 95% HPD interval when using the UCLN model for inference than the strict clock model for inference. However, the precision as measured by the total width of the 95% HPD interval for the UCLN runs were much lower than the clock runs (see Tables 4-5). Those nodes that were not within the interval of the 95% HPD when using the strict clock model for reconstruction, were close to the true value. So, while fewer true node ages were contained in the strict clock HPDs, the overall error rate was lower. For example, in the CARY dataset, while fewer nodes in the clock estimate were found to be within the interval (52 vs 67 for the UCLN), the distance of the interval from the estimate was lower for the clock dataset for both the high and low value for the 95% HPD. Stated another way, the UCLN intervals were large enough that the true age was often included, but this was at the cost of far lower precision. Because of this error relative to the strict clock, the UCLN perhaps should not be the preferred model, especially if the researcher is going to use a single summary tree for future analyses.

Several gene trees from the examples discussed fail a standard strict clock test but have low tip-to-root variance. To explore this further, we simulated strict clock amino acid and nucleotide data on orthologs from each empirical dataset and examined the frequency of incorrectly rejecting a strict clock. The false rejection rate for clock tests using amino acid data and a strict clock were between 5% and 8%. For the two nucleotide datasets, the rejection rate was much higher at 23% and 46%. This suggests that for amino acid data, the false rejection rate was near the nominal value, while for the nucleotide datasets the false rejection rate was unreliable. Both nucleotide datasets (BIR and CARY) also had the largest number of species and so the rejection rate may be a function of the number of

298 taxa. Sensitivity of the clock-test to nucleotide data is not the focus of this study, but
299 should be examined in more detail. Also, it would be more informative to examine the
300 deviation from the clock instead of a boolean test of significant fit. In regard to divergence
301 time estimation, if a strict or stricter clock can be used, molecular phylogenies may be
302 dated with significantly lower error. As an added benefit, fewer fossils would be necessary
303 to calibrate nodes (and indirectly, rates). We suggest that the community explore model fit
304 to relaxed clock models as well as potential alternatives to the prevailing strict clock test
305 that may be more beneficial for divergence time estimates and more informative in regard
306 to rate heterogeneity in phylogenomic datasets.

307 ## *Acknowledgements*

308 We would like to thank Oscar Vargas, Greg Stull, Jianjun Jin, Drew Larson, Ning Wang,
309 Caroline Parins-Fukuchi, Edwige Moyroud, and Lijun Zhao for discussion of the
310 manuscript and method. JFW and SAS were supported by NSF 1354048. JWB and SAS
311 were supported by NSF 1207915.

312 ## *Data availability*

313 All unpublished analyses and datasets are available through Data Dryad (#XXXXXX).
314 Associated scripts related to the method are available on GitHub.

315 ## *Author contributions*

316 SAS, JWB, and JFW conceived of the project. SAS and JFW analyzed the data. SAS,
317 JWB, and JFW wrote the manuscript.

318 *

319 References

320 Anisimova, M. and Gascuel, O. 2006. Approximate likelihood-ratio test for branches: A
321 fast, accurate, and powerful alternative. *Systematic Biology*, 55(4): 539–552.

322 Beaulieu, J. M., O'Meara, B. C., Crane, P., and Donoghue, M. J. 2015. Heterogeneous
323 rates of molecular evolution and diversification could explain the triassic age estimate for
324 angiosperms. *Systematic Biology*, 64(5): 869–878.

325 Brewer, M. S. and Bond, J. E. 2013. Ordinal-level phylogenomics of the arthropod class
326 diplopoda (millipedes) based on an analysis of 221 nuclear protein-coding loci generated
327 using next-generation sequence analyses. *PLOS ONE*, 8(11).

328 Brown, J. W., Walker, J. F., and Smith, S. A. 2017. phyx: Phylogenetic tools for unix.
329 *Bioinformatics*. accepted.

330 Dornburg, A., Brandley, M. C., McGowen, M. R., and Near, T. J. 2012. Relaxed clocks
331 and inferences of heterogeneous patterns of nucleotide substitution and divergence time
332 estimates across whales and dolphins (mammalia: Cetacea). *Molecular Biology and*
333 *Evolution*, 29(2): 721–736.

334 Drummond, A. J. and Rambaut, A. 2007. BEAST: Bayesian evolutionary analysis by
335 sampling trees. *BMC Evolutionary Biology*, 7(1): 214.

336 Drummond, A. J. and Suchard, M. A. 2010. Bayesian random local clocks, or one rate to
337 rule them all. *BMC Biology*, 8(1): 114.

338 Drummond, A. J., Ho, S. Y., Phillips, M. J., Rambaut, A., *et al.* 2006. Relaxed
339 phylogenetics and dating with confidence. *PLoS Biology*, 4(5): 699.

340 Fletcher, W. and Yang, Z. 2009. Indelible: a flexible simulator of biological sequence
341 evolution. *Molecular Biology and Evolution*, 26(8): 1879–1888.

342 Gatesy, J. and Springer, M. S. 2014. Phylogenetic analysis at deep timescales: Unreliable
343 gene trees, bypassed hidden support, and the coalescence/concatalescence conundrum.
344 *Molecular Phylogenetics and Evolution*, 80: 231 – 266.

345 Heath, T. A., Huelsenbeck, J. P., and Stadler, T. 2014. The fossilized birth–death process
346 for coherent calibration of divergence-time estimates. *Proceedings of the National*
347 *Academy of Sciences*, 111(29): E2957–E2966.

348 Heled, J. and Drummond, A. J. 2015. Calibrated birth–death phylogenetic time-tree priors
349 for bayesian inference. *Systematic Biology*, 64(3): 369–383.

350 Ho, S. Y. W., Duchêne, S., and Duchêne, D. 2015. Simulating and detecting
351 autocorrelation of molecular evolutionary rates among lineages. *Molecular Ecology*
352 *Resources*, 15(4): 688–696.

353 Jarvis, E., Mirarab, S., Aberer, A., Houde, P., Li, C., Ho, S., Faircloth, B., Nabholz, B.,
354 Howard, J., Suh, A., Weber, C., Fonseca, R., Alfaro-Nunez, A., Narula, N., Liu, L., Burt,
355 D., Ellegren, H., Edwards, S., Stamatakis, A., Mindell, D., Cracraft, J., Braun, E.,
356 Warnow, T., Jun, W., Gilbert, M., and Zhang, G. 2014a. Phylogenomic analyses data of
357 the avian phylogenomics project.

358 Jarvis, E. D., Mirarab, S., Aberer, A. J., Li, B., Houde, P., Li, C., Ho, S. Y. W., Faircloth,
359 B. C., Nabholz, B., Howard, J. T., Suh, A., Weber, C. C., da Fonseca, R. R., Li, J.,
360 Zhang, F., Li, H., Zhou, L., Narula, N., Liu, L., Ganapathy, G., Boussau, B., Bayzid,
361 M. S., Zavidovych, V., Subramanian, S., Gabaldón, T., Capella-Gutiérrez, S.,
362 Huerta-Cepas, J., Rekepalli, B., Munch, K., Schierup, M., Lindow, B., Warren, W. C.,
363 Ray, D., Green, R. E., Bruford, M. W., Zhan, X., Dixon, A., Li, S., Li, N., Huang, Y.,
364 Derryberry, E. P., Bertelsen, M. F., Sheldon, F. H., Brumfield, R. T., Mello, C. V.,
365 Lovell, P. V., Wirthlin, M., Schneider, M. P. C., Prosdocimi, F., Samaniego, J. A.,
366 Velazquez, A. M. V., Alfaro-Núñez, A., Campos, P. F., Petersen, B., Sicheritz-Ponten,
367 T., Pas, A., Bailey, T., Scofield, P., Bunce, M., Lambert, D. M., Zhou, Q., Perelman, P.,

368 Driskell, A. C., Shapiro, B., Xiong, Z., Zeng, Y., Liu, S., Li, Z., Liu, B., Wu, K., Xiao, J.,
369 Yinqi, X., Zheng, Q., Zhang, Y., Yang, H., Wang, J., Smeds, L., Rheindt, F. E., Braun,
370 M., Fjeldsa, J., Orlando, L., Barker, F. K., Jønsson, K. A., Johnson, W., Koepfli, K.-P.,
371 O'Brien, S., Haussler, D., Ryder, O. A., Rahbek, C., Willerslev, E., Graves, G. R.,
372 Glenn, T. C., McCormack, J., Burt, D., Ellegren, H., Alström, P., Edwards, S. V.,
373 Stamatakis, A., Mindell, D. P., Cracraft, J., Braun, E. L., Warnow, T., Jun, W., Gilbert,
374 M. T. P., and Zhang, G. 2014b. Whole-genome analyses resolve early branches in the
375 tree of life of modern birds. *Science*, 346(6215): 1320–1331.

376 Johnson, B. R., Borowiec, M. L., Chiu, J. C., Lee, E. K., Atallah, J., and Ward, P. S. 2013.
377 Phylogenomics resolves evolutionary relationships among ants, bees, and wasps. *Current*
378 *Biology*, 23(20): 2058 – 2062.

379 Ksepka, D. T., Parham, J. F., Allman, J. F., Benton, M. J., Carrano, M. T., Cranston,
380 K. A., Donoghue, P. C. J., Head, J. J., Hermsen, E. J., Irmis, R. B., Joyce, W. G., Kohli,
381 M., Lamm, K. D., Leehr, D., Patané, J. L., Polly, P. D., Phillips, M. J., Smith, N. A.,
382 Smith, N. D., Van Tuinen, M., Ware, J. L., and Warnock, R. C. M. 2015. The fossil
383 calibration database—a new resource for divergence dating. *Systematic Biology*, 64(5):
384 853–859.

385 Lepage, T., Bryant, D., Philippe, H., and Lartillot, N. 2007. A general comparison of
386 relaxed molecular clock models. *Molecular Biology and Evolution*, 24(12): 2669–2680.

387 Mirarab, S., Bayzid, M. S., Boussau, B., and Warnow, T. 2014. Statistical binning enables
388 an accurate coalescent-based estimation of the avian tree. *Science*, 346(6215).

389 Parham, J. F., Donoghue, P. C. J., Bell, C. J., Calway, T. D., Head, J. J., Holroyd, P. A.,
390 Inoue, J. G., Irmis, R. B., Joyce, W. G., Ksepka, D. T., Patané, J. S. L., Smith, N. D.,
391 Tarver, J. E., van Tuinen, M., Yang, Z., Angielczyk, K. D., Greenwood, J. M., Hipsley,
392 C. A., Jacobs, L., Makovicky, P. J., Müller, J., Smith, K. T., Theodor, J. M., Warnock,
393 R. C. M., and Benton, M. J. 2012. Best practices for justifying fossil calibrations.
394 *Systematic Biology*, 61(2): 346–359.

395 Prum, R. O., Berv, J. S., Dornburg, A., Field, D. J., Townsend, J. P., Lemmon, E. M., and
396 Lemmon, A. R. 2015. A comprehensive phylogeny of birds (aves) using targeted
397 next-generation dna sequencing. *Nature*, 526(7574): 569–573.

398 Roch, S. and Warnow, T. 2015. On the robustness to gene tree estimation error (or lack
399 thereof) of coalescent-based species tree methods. *Systematic Biology*, 64(4): 663–676.

400 Salichos, L., Stamatakis, A., and Rokas, A. 2014. Novel information theory-based measures
401 for quantifying incongruence among phylogenetic trees. *Molecular Biology and*
402 *Evolution*, 31(5): 1261–1271.

403 Sanderson, M. J. 2002. Estimating absolute rates of molecular evolution and divergence
404 times: a penalized likelihood approach. *Molecular Biology and Evolution*, 19(1): 101–109.

405 Sanderson, M. J. 2003. r8s: inferring absolute rates of molecular evolution and divergence
406 times in the absence of a molecular clock. *Bioinformatics*, 19(2): 301–302.

407 Smith, S. A. and O'Meara, B. C. 2012. treepl: divergence time estimation using penalized
408 likelihood for large phylogenies. *Bioinformatics*, 28(20): 2689–2690.

409 Smith, S. A., Beaulieu, J. M., and Donoghue, M. J. 2010. An uncorrelated relaxed-clock
410 analysis suggests an earlier origin for flowering plants. *Proceedings of the National*
411 *Academy of Sciences*, 107(13): 5897–5902.

412 Smith, S. A., Moore, M. J., Brown, J. W., and Yang, Y. 2015. Analysis of phylogenomic
413 datasets reveals conflict, concordance, and gene duplications with examples from animals
414 and plants. *BMC Evolutionary Biology*, 15(1): 150.

415 Stamatakis, A. 2014. Raxml version 8: a tool for phylogenetic analysis and post-analysis of
416 large phylogenies. *Bioinformatics*, 30(9): 1312–1313.

417 Swofford, D. L. 2001. PAUP*: Phylogenetic Analysis Using Parsimony (* and other
418 methods) 4.0.b5.

Tamura, K., Battistuzzi, F. U., Billing-Ross, P., Murillo, O., Filipski, A., and Kumar, S. 2012. Estimating divergence times in large molecular phylogenies. *Proceedings of the National Academy of Sciences*, 109(47): 19333–19338.

Walker, J. F., Yang, Y., Moore, M. J., Mikenas, J., Brockington, S. F., Timoneda, A., and Smith, S. A. 2017. Widespread paleopolyploidy, gene tree conflict and recalcitrant relationships among the carnivorous caryophyllales. *New Phytologist*. in review.

Wen, J., Xiong, Z., Nie, Z.-L., Mao, L., Zhu, Y., Kan, X.-Z., Ickert-Bond, S. M., Gerrath, J., Zimmer, E. A., and Fang, X.-D. 2013. Transcriptome sequences resolve deep relationships of the grape family. *PLOS ONE*, 8(9).

Worobey, M., Han, G.-Z., and Rambaut, A. 2014. A synchronized global sweep of the internal genes of modern avian influenza virus. *Nature*, 508: 254–257.

Yang, Y., Moore, M. J., Brockington, S. F., Soltis, D. E., Wong, G. K.-S., Carpenter, E. J., Zhang, Y., Chen, L., Yan, Z., Xie, Y., Sage, R. F., Covshoff, S., Hibberd, J. M., Nelson, M. N., and Smith, S. A. 2015. Dissecting molecular evolution in the highly diverse plant clade caryophyllales using transcriptome sequencing. *Molecular Biology and Evolution*.

Zhu, T., Dos Reis, M., and Yang, Z. 2015. Characterization of the uncertainty of divergence time estimation under relaxed molecular clock models using multiple loci. *Systematic Biology*, 64(2): 267–280.

437

Tables

Dataset	Orthologs	Clocklike (%)	
BIR	7116	440	(6.18)
CAR	3767	274	(7.27)
CARY	583	3	(0.51)
HYM	1161	22	(1.89)
MIL	152	26	(17.10)
VIT	2267	8	(0.35)

Table 1: Dataset size and results of likelihood ratio tests for strict clock-like gene behavior.

Gene name	Variance	Tree length	Bipartition proportion
BIR			
12969	0.000791644	2.73068	0.5
1173	0.00205589	3.01712	0.457
12123	8.32228e-05	0.825943	0.413
CAR			
cluster259MIortho7	9.07832e-05	0.346618	1.0
cluster3790MIortho1	0.000245644	0.739886	1.0
cluster234MIortho1	0.0004849	1.19575	1.0
CARY			
cc7674-1-1to1ortho	0.0183029	10.9821	0.701
cc4427-1MIortho1	0.0093838	8.7827	0.657
cc7873-1MIortho1	0.0206222	10.4773	0.657
HYM			
cluster3024-1-1ortho1	0.00159156	2.64137	0.706
cluster5160-1-1ortho1	0.00294197	2.0815	0.706
cluster1251-1-1ortho1	0.00621115	4.99913	0.706
MIL			
cluster89-1-1ortho1	0.00200945	0.909593	0.875
cluster1437-1-1ortho1	0.00872612	2.96511	0.875
cluster1615-1-1ortho1	0.010942	3.56434	0.875
VIT			
cluster9579-1MIortho1	0.000978163	0.519373	1.0
cluster1236-1MIortho1	0.00106778	0.547562	1.0
cluster461-1MIortho1	0.001227	0.607536	1.0

Table 2: Properties of the genes used in the empirical dating analyses. Variance regards the root-to-tip paths. Tree length is measured in units of expected substitutions per site across all branches. Bipartition proportion measures agreement to the species tree topology (1.0 indicates complete concordance).

Dataset	Height	Lower	Higher
BIR	-0.26	0.27	-1.49
CAR	-0.004	0.04	-0.2
CARY	-3.93	0.52	-8.56
HYM	-0.12	0.1	-0.63
MIL	-0.09	0.04	-1.12
VIT	-0.02	0.08	-0.56

Table 3: The cumulative difference in the height, lower 95% HPD, and higher 95% HPD of each node comparing the UCLN estimates to the clock estimates from the individual empirical dating analyses. A value lower than 0 results when the cumulative difference in the clock values of height or HPD are younger than the associated UCLN values.

	Height		Lower		Higher		Nodes		Error	
Dataset	CL	UC	CL	UC	CL	UC	CL	UC	CL	UC
BIR	0.63	0.5	0.48	0.69	0.96	1.33	16	39	1.44	2.02
CAR	0.26	0.2	0.37	0.85	0.25	0.63	5	12	0.62	1.49
CARY	0.54	0.63	1.23	2.12	0.64	1.11	52	67	1.88	3.24
HYM	0.16	0.76	0.21	0.65	0.38	0.94	15	3	0.58	1.59
MIL	0.17	0.42	0.12	0.45	0.33	0.46	5	3	0.44	0.91
VIT	0.27	0.26	0.42	0.32	0.2	0.27	5	8	0.62	0.59

Table 4: Assessment of dating error for the clock (CL) and UCLN (UC) analyses of the simulated *clock* data. All measures involve distance from the true node age, and are cumulative sums across all nodes. Height is the inferred node age. Lower and Higher regard the 95% HPD node age bounds. Nodes indicates the number of true node ages contained within the HPD interval. Error is the total error involved, equivalent to Low + High.

	Height		Lower		Higher		Nodes		Error	
Dataset	CL	UC	CL	UC	CL	UC	CL	UC	CL	UC
BIR	1.26	3.21	1.26	6.43	1.37	1.52	12	24	2.64	7.95
CAR	0.76	0.69	0.89	1.59	0.68	0.58	2	9	1.57	2.17
CARY	2.29	3.51	2.37	8.98	2.38	4.97	15	55	4.75	13.95
HYM	0.14	0.91	0.61	3.01	0.61	1.58	18	16	1.22	4.65
MIL	0.14	0.61	0.32	1.6	0.57	1.17	11	10	0.89	2.77
VIT	0.29	1.12	0.82	2.43	0.29	0.73	14	9	1.11	3.16

Table 5: Assessment of dating error for the clock (CL) and UCLN (UC) analyses of the simulated *ucln* data. All measures involve distance from the true node age, and are cumulative sums across all nodes. Height is the inferred node age. Lower and Higher regard the 95% HPD node age bounds. Nodes indicates the number of true node ages contained within the HPD interval. Error is the total error involved, equivalent to Low + High.

438

Figures and Figure captions

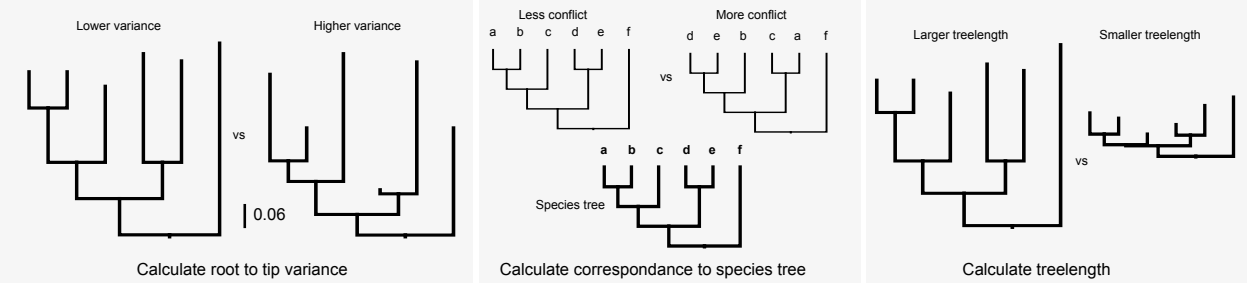

Figure 1: Measures used for sorting genes for use in dating analyses. The order presented here is arbitrary.

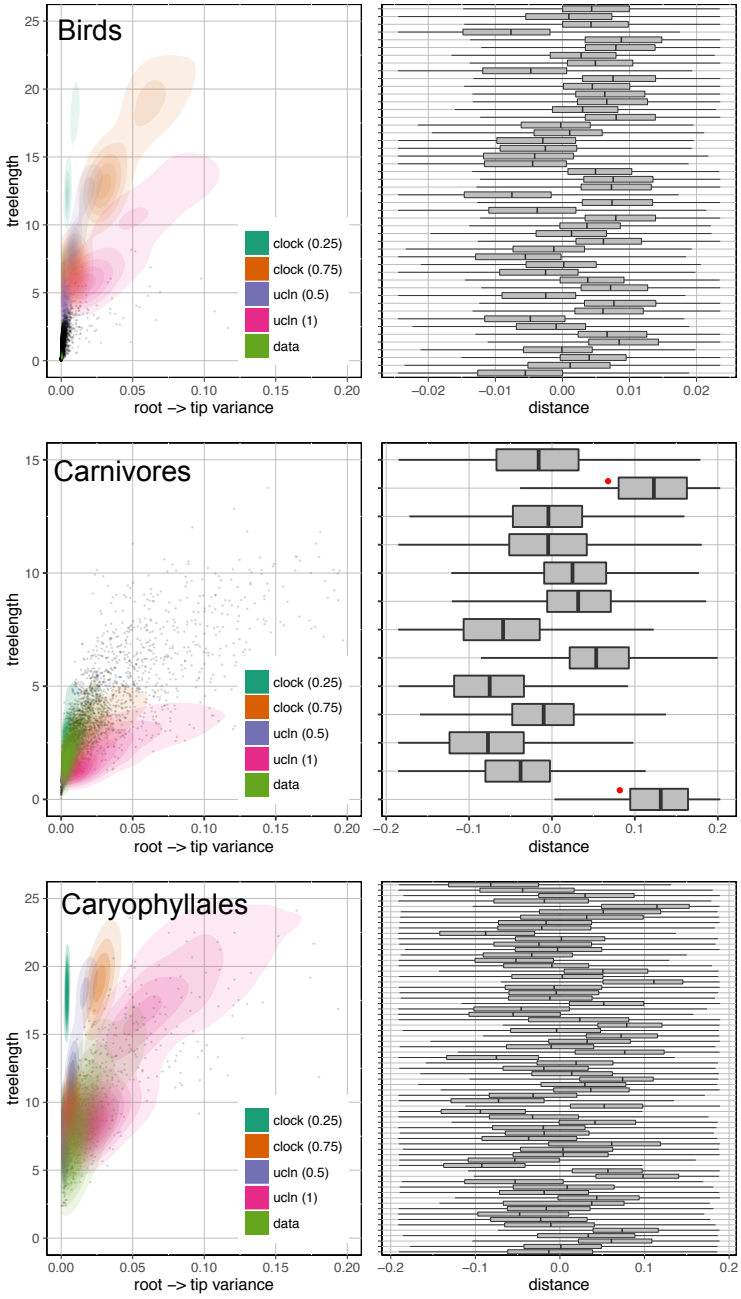

Figure 2: Plots of gene tree properties (left, including root-to-tip variance and treelength for simulated and empirical datasets) and tip-specific root-to-tip variance for empirical datasets (right). When the outgroup is present, the taxa are labeled with a red dot.

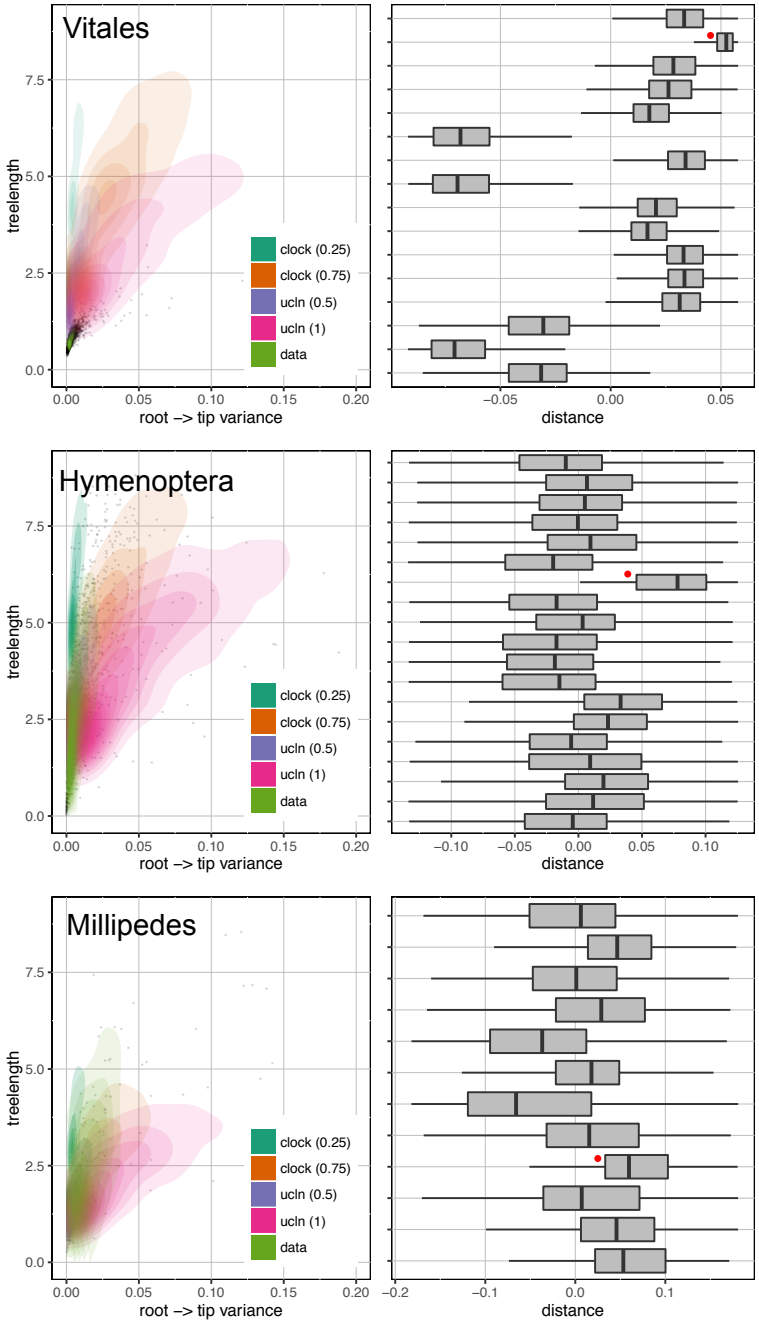

Figure 3: Plots of gene tree properties (left, including root-to-tip variance and treelength for simulated and empirical datasets) and tip-specific root-to-tip variance for empirical datasets (right). When the outgroup is present, the taxa are labeled with a red dot.

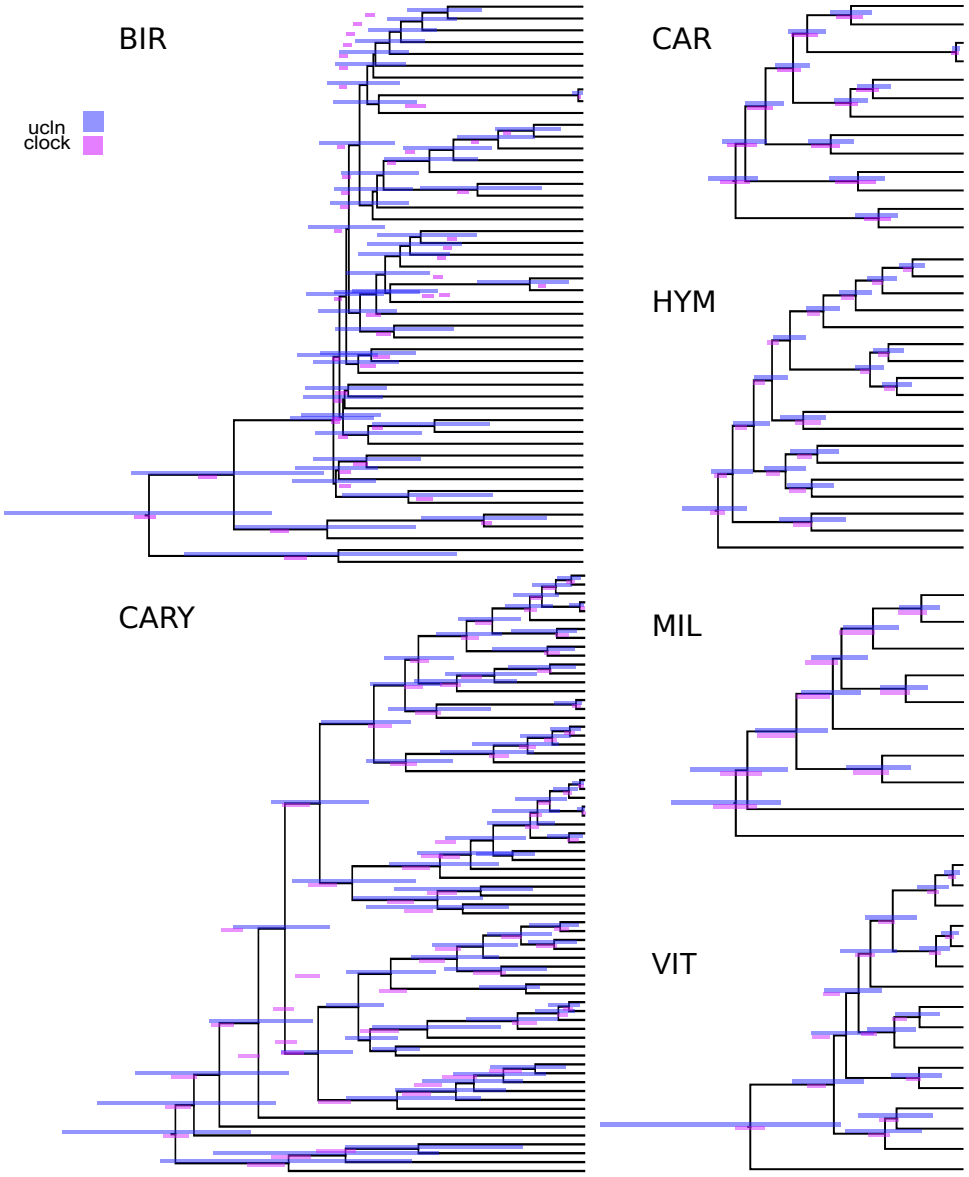

Figure 4: A comparison of strict clock and UCLN estimates of node ages for the six curated empirical datasets.

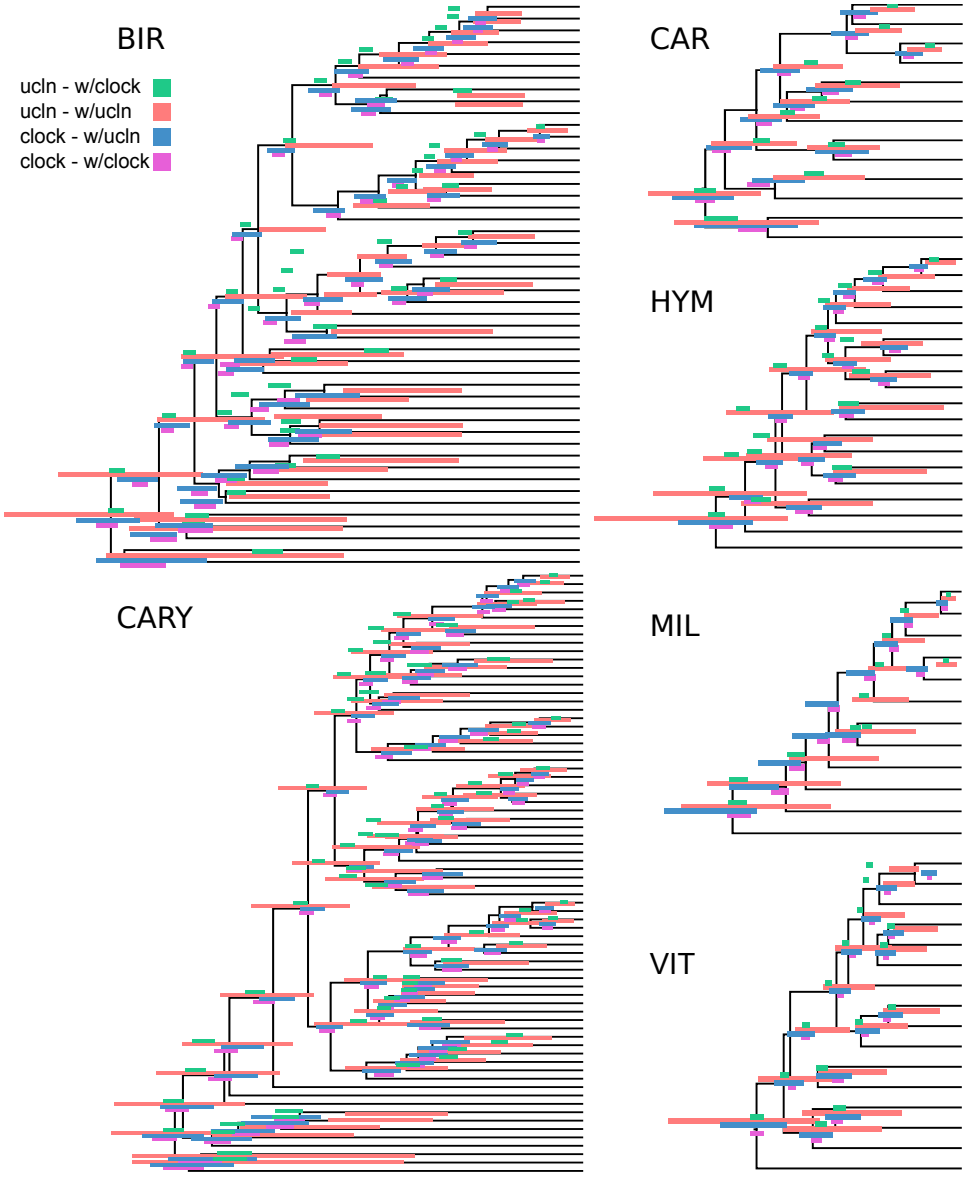

Figure 5: A comparison of strict clock and UCLN estimates of node ages for the simulated *clock* and *ucln* datasets. Red and pink are scenarios where the generating and inference are identical, while green and blue are where the models are mismatched.